https://doi.org/10.5194/acp-2022-680
Preprint. Discussion started: 10 October 2022

Atmospheric Chemistry and Physics Discussions

Indicators of the ozone recovery for selected sites in the Northern Hemisphere mid-latitudes derived from various total column ozone datasets (1980–2020)

Janusz Krzyścin[1]

[1]Institute of Geophysics, Polish Academy of Sciences, Warsaw, 01-452, Poland

Correspondence to: Janusz Krzyścin (jkrzys@igf.edu.pl)

Abstract. We propose a method to examine the current status of the ozone recovery attributed to ozone-depleting substances (ODS) changes in the stratosphere. The total column ozone (TCO_3) datasets used are based on the ground-based (by the Dobson and/or Brewer spectrophotometer) measurements, satellite observations (from the Solar Backscatter Ultraviolet, SBUV, and Ozone Mapping and Profiler Suite, OMPS, instrument), and output of reanalyzes (Multi-Sensor Reanalysis version 2, MSR2, and Modern-Era Retrospective Analysis for Research and Applications, version 2, MERRA2). The TCO_3 time series are calculated for selected sites in the NH mid-latitudes (35°N–60°N), which are station locations with long-term TCO_3 observations archived at the World Ozone and Ultraviolet Radiation Data Centre (WOUDC). The TCO_3 monthly means (1980–2020) are averaged over the April–September period to obtained TCO_3 time series for the warm sub-period of the year. Two types of the averaged TCO_3 time series are considered: the original one and that with removed natural variability by a standard multiple regression model. TCO_3 time series were smoothed by the Locally Weighted Scatterplot Smoother (LOWESS) and the Super Smoother (SS). The smoothed TCO_3 values in 1980, 1988, 1997, and 2020 are used to build Ozone Recovery Indices (ORIs) in 2020. These are key years in the equivalent effective stratospheric chlorine (EESC) time series, i.e., the EESC minimum year when the stratosphere was only slightly contaminated by ODS, the year (before the ESSC maximum) with the EESC value equal to that at the end of the TCO_3 data, the EESC maximum year in the Northern Hemisphere mid-latitudes, and the end of TCO_3 data. The first proposed ORI, ORI_1, is the normalized difference between the TCO_3 values in 2020 and 1988. The second one, ORI_2, is the percentage of the recovered TCO_3 in 2020 since the ODS maximum. Following these definitions, the corresponding reference values, 0 % for ORI_1 and 51.7 % for ORI_2, are obtained from the EESC time series. The ozone recovery phases are classified comparing the current ORI values and their uncertainty ranges (by the bootstrapping) with the reference values. In the analyzed TCO_3 time series, for specific combinations of datasets, data types, and the smoother used, we find faster (ORI_1>0 % or ORI_2>51.7 %), slower (ORI_1<0 % or ORI_2<51.7 %) recovery in 2020 than that inferred from the EESC change, and a continuation of TCO_3 decline after the EESC peak (ORI_2<0 %). Using the original datasets, the strong signal of the slower TCO_3 recovery can be found in five stations: Nashville, Toronto, Hohenpeissenberg, Hradec Kralove, and Belsk. This is also in the series with removed proxy effects for those stations excluding Nashville. A continuation of ozone decline after the turnaround in ODS concentration is found both in the original and non-proxy time series from WOUDC (Toronto), SBUV&OMPS (Toronto, Arosa, Hohenpeissenberg, Uccle, Hradec Kralove, and Belsk), and MERRA2 data (Hohenpeissenberg, Hradec Kralove, and Belsk).

1 Introduction

Unexpected low total column ozone (TCO_3) values observed in the early 1980s over Antarctica alarmed both scientists and public because of anticipated increase of ultraviolet radiation (UVR) reaching the Earth surface (Chubachi, 1984; Farman et al., 1985; Solomon et al., 1986). Widespread threats of thinning of the stratospheric ozone layer and corresponding danger for the Earth environment led to signing the Montreal Protocol (MP) in 1987 to phaseout of the man-made ozone depleting substances (ODS). Overturning of the ODS concentration in the stratosphere (from large increase since the early 1980s to

https://doi.org/10.5194/acp-2022-680
Preprint. Discussion started: 10 October 2022

Atmospheric Chemistry and Physics Discussions

slight decrease beginning in the mid-1990s) was an evident sign of the success of MP and its subsequent amendments. The ODS turnaround in the stratosphere was observed around the middle 1990s in the mid-latitudes and at the beginning of the 2000s in Antarctica. This also triggered numerous studies to reveal the corresponding change point also in TCO_3 trends to support impact of the MP and its later amendments on the ozone layer (e.g., Reinsel et. al., 2005; Mäder et al., 2007; Harris et al., 2008; Weber et al., 2018).

Trends in ozone were usually calculated using multiple linear regression (MLR) with a number of proxies to eliminate TCO_3 variations related to dynamical oscillations in the atmosphere, and driven by the solar 11-year activity and volcanic eruptions. The anthropogenic component of the trend term was usually modelled as independent (disjoint) or dependent (joint) two lines drawn for the periods of increasing and decreasing ODS concentration in the stratosphere (e.g., Weber et al., 2018). There were only a few papers using a non-linear smoothed trend pattern based on dynamical linear model (Laine et al., 2014 and Maillard Barras et al., 2022), Fourier series (Bozhkova et al., 2019), and other smoothers, e.g., locally weighted scatterplot smoothing (LOWESS) by Krzyścin and Rajewska-Więch (2016) and wavelets by Delage et al. (2022).

Coldewey-Egbers et al. (2022) calculated longitude/longitude linear TCO_3 trends since 1995 over the entire globe based on the satellite data record. The trends in the NH mid-latitudes were mostly insignificant. In some isolated regions there, they found statistically significant trends, e.g., negative in East Europe and positive in the northern part of the North Atlantic. This pattern was linked with the opposite trends in the tropopause height. A continuation of the TCO_3 declining tendency since the ODS turnaround was surprisingly revealed in the NH lower stratosphere (Ball et al., 2018). Rather positive trend was expected due to a strengthening of the Brewer–Dobson circulation that was suggested by chemistry–climate models (e.g., Dietmüller et al. 2021). The negative trends in the NH lower stratosphere might be attributed to enhanced horizontal air mass exchange with the tropical region less abundant with ozone in the lower stratosphere (Thompson et al. 2021). However, other studies using observational data did not reveal such decline in the NH lower stratospheric ozone mostly due to large uncertainty in the satellite observations (e.g., Arosio et al. 2019).

NASA proposed the Ozone Depleting Gas Index (ODGI) to keep track on changes in ODS concentration in the mid-latitudes and Antarctica (Montzka et al., 2022). Equivalent effective stratospheric chlorine (EESC) was used as a measure of the stratospheric halogen loading, which is weighted by the ozone destruction potential of each gas depleting stratospheric ozone. ODGI was defined as an indicator of the EESC current decline since its peak that is expressed in percentage of the corresponding decline needed to reach the EESC level in 1980, when ODS concentration in the stratosphere was only slightly affected by man-made substances. The EESC peak year in the mid-latitude stratosphere was found in 1997 being three years later than the ODS peak in the troposphere (Montzka et al., 2022). The corresponding ODGI value in 2020 was 51.7 % providing almost half reduction of EESC necessary to reach its undisturbed level existing in 1980. This also provided an estimate of the recovery time around 2045 in the mid-latitudes if factors affecting ODS changes were the same as those in the period 1997–2020. In addition, the EESC level in 2020 corresponds to that of 1988 (Fig. 1).

Following ODGI concept, we propose indices to monitor ozone recovery attributed to the EESC changes using various TCO_3 dataset from ground-based and satellite observations, and two reanalyzes. These indices will be calculated for selected NH mid-latitudinal sites corresponding to locations of the ground-based stations with long-term time series archived in the World Ozone and Ultraviolet Radiation Data Centre (WOUDC). From the smoothed pattern of long-term TCO_3 changes, we will extract TCO_3 values in key years: 1980, 1988, 1997 and 2020 (Fig. 1). These four values will be used to calculate the proposed ozone recovery indices (ORIs) showing the current stage of the stratospheric ozone recovery.

In Sect. 2, the TCO_3 datasets are presented. In Sect. 3, the data preparation, ORI definition, and a method to obtain the uncertainty range of the ORI estimate are described. Section 4 presents ORI values for selected mid-latitudinal sites for various datasets using combination of the data smoother and data categories. In Sect. 5, the discussion and conclusions are presented.

https://doi.org/10.5194/acp-2022-680
Preprint. Discussion started: 10 October 2022

Atmospheric Chemistry and Physics Discussions

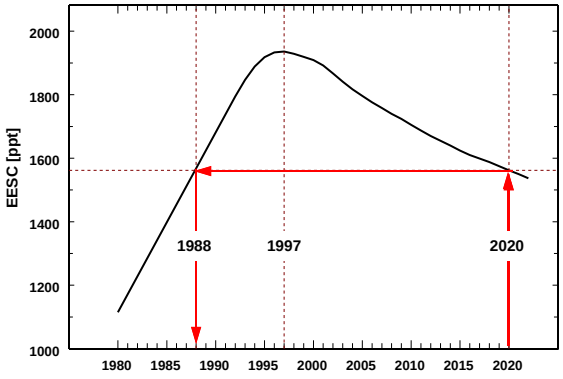

Figure 1: The EESC time series with marked key years: the EESC maximum in 1997 and 1988 when the EESC value was the same as in 2020 (the end of total column data used in the paper).

2 Total column ozone datasets

Four TCO_3 data sets are used in the study based on the ground-based and satellite observations as well as from two reanalyzes. The TCO_3 time series are calculated for selected sites in the NH mid-latitudes (35°N–60°N) corresponding to locations of stations that archived results of the ground-based observations by the Dobson and/or Brewer spectrophotometer at WOUDC. Arosa and Davos data sets are combined as the ozone monitoring at Arosa was moved to nearby station Davos in 2014. 16 stations with long-term and continuous observations (starting at least before 1980 and ending after 2020) are selected (Table 1). The monthly mean TCO_3 values for these stations are taken from the WOUDC web site.

The NASA Merged Ozone Data (MOD) version 8.7 is used for a comparison with the WOUDC data. Overpass subset of MOD provides daily means of ozone content in various stratospheric layers and column ozone over the WOUDC sites including also those listed in Table 1. MOD time series are build using the homogenized spectral measurements of the solar backscattered UV on various satellite platforms Nimbus 4, Nimbus 7, NOAA 9, 11, 14, 16, and 17–19, and Suomi National Polar-orbiting Partnership (NPP) (Weber et al., 2022).

Table 1: Selected ground-based total column ozone observing stations in the NH midlatitudes with the data record archived in WOUDC.

No.	WOUDC No.	Station	Lat.	Lon.	Elevation
		Japan			
1	14	Tateno	36.0°N	140.1°E	31 m
2	12	Sapporo	43.1°N	141.3°E	19 m
		North America			
3	106	Nashville	36.3°N	86.6°W	182 m
4	67	Boulder	40.1°N	105.3°W	1689 m
5	65	Toronto	43.8°N	79.5°W	198 m
6	19	Bismarck	46.8°N	100.1°W	511 m
7	76	Goose Bay	53.3°N	60.4°W	40 m
8	21	Edmonton	53.6°N	114.1°W	766 m
9	77	Churchill	58.8°N	94.1°W	35 m
		Europe			
10	35	Arosa	46.8°N	9.7°E	1840 m
11	99	Hohenpeissenberg	47.8°N	11.0°E	975 m
12	96	Hradec Kralove	50.2°N	15.9°E	285 m
13	53	Uccle	50.8°N	4.4°E	100 m
14	68	Belsk	51.8°N	20.8°E	180 m
15	165	Oslo	59.9°N	10.7°E	90 m
16	43	Lerwick	60.0°N	1.2°W	80 m

https://doi.org/10.5194/acp-2022-680
Preprint. Discussion started: 10 October 2022

Atmospheric Chemistry and Physics Discussions

Other two data sets represent the category of reanalyzed data, i.e., global TCO_3 field taken from output of 3-D chemistry and transport model (CTM). Here we examine time series for the selected sites interpolated from the Multi-Sensor Reanalysis, version 2 (MSR2) global data with the 0.5° x 0.5° resolution (van der A et al., 2015) and Modern-Era Retrospective analysis for Research and Applications, version 2 (MERRA2) with the 0.5° (latitude)x 0.625°(longitude) resolution (Wargan et al., 2017). Table 2 present the sources of all data sets used in the study.

Table 2: Source of total column ozone datasets.

Datasets	Time Resolution	Data Start	WEB Page
WOUDC	Day	1926 (Arosa)	https://woudc.org/archive/Summaries/TotalOzone/Daily_Summary/
MOD	Day	1970	https://acd-ext.gsfc.nasa.gov/anonftp/toms/sbuv/MERGED/
MSR2	Month	1979	http://climexp.knmi.nl/select.cgi?field=o3col
MERRA2	Month	1980	https://disc.gsfc.nasa.gov/datasets/M2TMNXCHM_5.12.4/summary

3 Methods

The TCO_3 monthly means from all data sets described in Sect. 2 are averaged over warm sub-period of the year (April–September) to build seasonal TCO_3 time series (1980–2020) for all NH mid-latitudinal selected sites listed in Table 1. TCO_3 observations by the spectrometers are the most accurate in this part of the year because of high solar elevations allowing AD observations by the Dobson instrument (Komhyr, 1980). During the warm sub-period of the year, UVR is much higher comparing to the cold sub-period. UV overexposures having detrimental effect on the Earth ecosystems are most frequent in the warm sub-period of the year. Therefore, analysis of the long-term TCO_3 changes in this period of the year is of special importance to discuss detrimental biological effects of the ozone changes. In the mid-1980s, the anticipated risks of UV overexposure led to international initiatives to protect the ozone layer.

3.1 Data smoother

Two data smoother types are examined in the study: LOWESS by Cleveland (1979) and super smoother (SS) by Friedman (1984). Here, for LOWESS application, the smoothness level is pre-defined to have up to two turning points in the smoothed time series, i.e., the smoothing parameter *f* is set equal to 0.5. The first turning point corresponds to the ODS turning point in 1997 and next point is to reveal a change of the recovery rate after 1997 (if it exists). For SS, we use an option with not pre-defined smoothness level. The smoothed curve is obtained by means of a bivariate regression smoother based on local linear regression with adaptive bandwidths. Figure 2 illustrates the performance of both smoothers applied to the time series of seasonal (April–September) TCO_3 means for Tateno and Toronto.

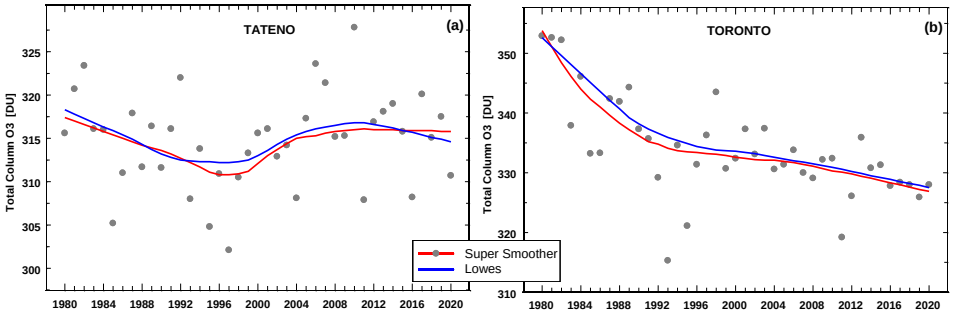

https://doi.org/10.5194/acp-2022-680
Preprint. Discussion started: 10 October 2022

Atmospheric Chemistry and Physics Discussions

Figure 2. Examples of the long-term time series of total column ozone in the warm sub-period (April–September) of the year by locally weighted scatterplot smoother (Lowess -blue curve) and super smoother (red curve): Tateno (a), Toronto (b).

3.2 Removal of the ozone natural variability

The smoothed pattern of TCO_3 time series is used to discuss long-term variability in the series comprising 41 yearly values. The smoothers described in Sect. 3.1 are applied to both original time series and the series with removed variability due to various dynamical/chemical processes not directly involved with the anthropogenic emission of chemicals affecting the stratospheric ozone. Various proxies (explanatory variables in MLR regressions) for these "natural" processes have been proposed parameterizing dynamical/chemical forcing on the ozone layer. Frequently in MLR, the solar activity cycle (e.g., 10.7 cm solar radio flux), indices of internal atmospheric fluctuations (Quasi Biennial Oscillations, El-Nino Southern Oscillation, and Arctic Oscillation), optical depth of the stratospheric aerosols, and the eddy heat flux in the stratosphere (to parameterize the intensity in the Brewer-Dobson circulation) were used. The proxy set proposed by Weber et al. (2022) is used here with the sources listed in their Table 2. The only differences between our and Weber et. (2022) proxy set is using the eddy heat flux at 100 hPa from the NASA Atmospheric Chemistry and Dynamics Laboratory data base (https://acd-ext.gsfc.nasa.gov/Data_services/met/ann_data.html) and the stratospheric aerosol optical depth updated from Sato et al. (1993) for the entire time data (i.e., no different aerosol data sources after 1990).

The standard MLR with two independent linear trend terms (before and after the year of ODS turnaround) is used to extract the trend pattern and the combined signal due to all proxies. The MLR used here is identical to the one labeled as full MLR in Weber et. (2022). Finally, the explained part of TCO_3 variability related to the combined proxy effects is subtracted from the original time series to obtain the TCO_3 series comprising only the anthropogenic long-term component and noise.

3.3 Ozone Recovery Index

The proposed ozone recovery indices (ORIs) follow the ODGI concept (Montzka et al., 2022) of using selected values from the EESC series to define the recovery status. Key TCO_3 values are taken at the beginning (1980), at the end of the data (2020), in the year of TCO_3 trend overturing (1997), and in the year (1988) when the EESC value in the NH mid-latitudes was the same as at the end year. Namely, smoothed TCO_3 values in the selected key years T, denoted as $< TCO_3(T) >$, T={1980, 1988, 1997, 2020}, are used for calculation of the following dimensionless ORIs in 2020:

$$ORI_1(2020) = 100\% \frac{< TCO_3(2020) > - < TCO_3(1988) >}{< TCO_3(1980) >} \quad (1)$$

$$ORI_2(2020) = 100\% \frac{< TCO_3(2020) > - < TCO_3(1997) >}{< TCO_3(1980) > - < TCO_3(1997) >} \quad (2)$$

If the ozone recovery follows ODS changes, $ORI_1(2020)$ will be equal to 0 % but negative (positive) for slower (faster) TCO_3 recovery than that found in the EESC pattern. Correspondingly, $ORI_2(2020)$ value in the Northern Hemisphere will be equal to 51.7 % if the ozone recovery in the period 1980-2020 follows EESC changes and lower (higher) than this reference value if the ozone recovery is slower (faster) comparing to that found in the EESC. If $ORI_2(2020)$ is less than 0 % and the ozone is declining before the ODS overturning year (usual case of the NH mid-latitudinal TCO_3), the ozone depletion will continue throughout the period 1980-2020.

To calculate $ORI_1(T1)$ in the NH mid-latitudes in any year $T1$ (>1997), the year $T2$ (<1997) when $ODS(T2) = ODS(T1)$ needs to be delineated from ODS pattern. In this case, the general formulas for ORIs are as follows:

$$ORI_1(T1) = 100\% \frac{< TCO_3(T1) > - < TCO_3(T2) >}{< TCO_3(1980) >} \quad (3)$$

https://doi.org/10.5194/acp-2022-680
Preprint. Discussion started: 10 October 2022

Atmospheric Chemistry and Physics Discussions

$$ORI_2(T1) = 100\% \frac{< TCO_3(T1) > - < TCO_3(1997) >}{< TCO_3(1980) > - < TCO_3\ (1997) >} \quad (4)$$

The ozone recovery will happen in the year *TR* when <$TCO_3(TR)$> = <TCO_3(1980)>. This means that the ozone recovered to its initial level when the stratosphere was not contaminated by man-made compounds (in 1980). In this case, ORI_2 (*TR*)=100 %. Negative ORI_2 (*T*1) values will be found when the ozone decline, which was observed in the period 1980-1997 (i.e., <TCO_3(1980)> – <TCO_3(1997)> is always positive), continues after 1997. It is worth mentioning that for a searching of the TCO_3 recovery over Antarctica in 2020, the smoothed TCO_3 values in 1980, 1993, 2001, and 2020 need to be selected as these years correspond with key years in the EESC pattern for this region (Montzka et al., 2022).

3.4 Uncertainty of ORI estimates

The original TCO_3 time series in year *t*, $TCO_3(t)$ is divided into two parts to account for the long-term variability, <TCO_3(t)>, which is extracted by the smoother, and the residual parts, $Resid\_TCO_3(t)$:

$$TCO_3(t) = < TCO_3(t) > + Resid\_TCO_3(t) \quad (5)$$

For each selected WOUDC station and data types (original and without proxy effects), two smoothers (LOWESS and SS) are applied to extract the long-term variability and the residual part of TCO_3 variability comprising dynamical/chemical part of variations and noise. The uncertainty range (between the 5th and the 95th percentile) of each ORI estimate is calculated from the set of ordered (lowest to highest) synthetic ORI values derived by bootstrapping. This method of calculations uncertainties of the trend estimates has been applied in our previous studies (e.g., Krzyścin et al., 2015).

First step of bootstrapping is building synthetic *n*-th time series, $Resid_{TCO_3^n(t)}$, to mimic the residual term in Eq. (5),

$$Resid\_TCO_3^n(t) = Resid\_TCO_3(t_x), \qquad t_x \epsilon \{1980, \dots, 2020\}, \quad n = \{1, \dots, N\} \quad (6)$$

Random year t_x is obtained by drawing with replacement any year between 1980 and 2020. The total number of the bootstrapped time series used, *N*=10000, is derived experimentally to have stable estimates of ORIs. The use of the drawing with replacement in the construction of analytical residuals was allowed because the original residuals were random, which was confirmed by the Wald-Wolfowitz one sample run test (Wald and Wolfowitz, 1940).

The original and synthetic residuals should be identical in nature, i.e., have almost similar cumulative distribution. The Wald-Wolfowitz two samples run test is applied to check the difference between the original and synthetic residuals. If the time series of residuals derived by the drawing with replacement was found to be significantly different (at 5 % significance level) from the original ones, such the residuals were not used in the bootstrapping. This means that the number of draws was greater than the total number of the series (*N*) used in the bootstrap sample.

Next step of the bootstrapping is adding $Resid\_TCO_3^n$ term to the smoothed part of the original TCO_3 series to build *n*-th synthetic TCO_3 time series:

$$TCO_3^n(t) = < TCO_3(t) > + Resid\_TCO_3^n(t) \quad (7)$$

The smoothed n-th time series, $< TCO_3^n(t) >$ is obtained applying LOWESS (or SS) to synthetic $TCO_3^n(t)$ time series. Repeating this procedure, a set of synthetic series, $TCO_3^n(t),\ n = \{1, \dots N\}$, is constructed.

Finally, for each $< TCO_3^n(t) >$ series, $ORI_1^n(2020)$ and $ORI_2^n(2020)$ are calculated using Eq. (1) and Eq. (2), respectively. From the ordered set of $ORI_1^n(2020)$ and $ORI_2^n(2020)$ values, the uncertainty range (5th percentile–95th percentile) is obtained. This allows to discuss if ORIs values are significantly different than the reference ORIs values defining the recovery stage, i.e., 0 % and 51.7 % for $ORI_1(2020)$ and $ORI_2(2020)$, respectively.

https://doi.org/10.5194/acp-2022-680
Preprint. Discussion started: 10 October 2022

Atmospheric Chemistry and Physics Discussions

4 Results

Figures 3–4 illustrate the median and uncertainty range of $ORI_1(2020)$ and $ORI_2(2020)$, respectively, for all WOUDC stations listed in Table 1. These values are calculated using TCO_3 monthly mean values averaged over the warm sub-period of the year. Results are shown in Figs. 3–4 (a–d) for WOUDC, MOD, MSR2, and MERRA2 data, respectively. The order of the stations on "x" axis in these Figures is the same as in Table 1, i.e., first there are two Japanese stations, then seven North American, and finally seven European stations. For each region (between the vertical dashed lines), the results are arranged from the southernmost to the northernmost station.

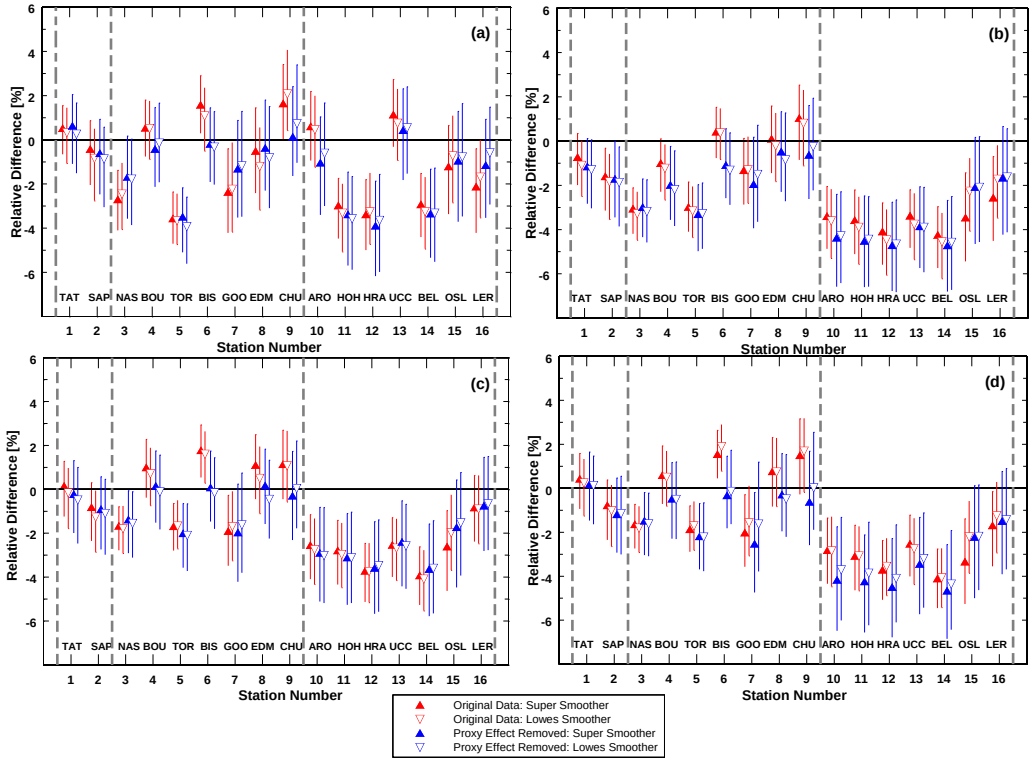

Figure 3. Median of the ozone recovery index, $ORI_1(2020)$, estimate (triangle) based on Eq. (1) and its uncertainty range (line) for 16 NH mid-latitudinal stations (Table 1) and various combination of data smoothers and datasets: WOUDC data (a), MOD data (b), MSR2 (c), and MERRA2 (d). Results in red are for the original data and in blue for the data with removed natural variability.

The location of the uncertainty range of ORIs in Figs. 3–4 relative to the horizontal reference lines provides the stage of the ozone recovery at each selected station. Namely, if the uncertainty range is entirely above (below) the horizontal reference lines, i.e., 0 %e for $ORI_1(2020)$ and 51.7% for $ORI_2(2020)$, the ozone recovery is faster (slower) than that found for the EESC change in the period 1980–2020. This means that the TCO_3 recovery rate is significantly different (at least at the 95 % confidence level) when compared with corresponding the EESC values. If the uncertainty range crosses the horizontal reference line, the hypothesis of the TCO_3 recovery rate similar to that in the EESC change cannot be rejected. The depletion

https://doi.org/10.5194/acp-2022-680
Preprint. Discussion started: 10 October 2022

Atmospheric Chemistry and Physics Discussions

of TCO_3 will continue even after the EESC maximum if the uncertainty range for $ORI_2(2020)$ is completely below 0 % reference line (dashed line in Fig. 4). In this case, there is no TCO_3 recovery between 1980 and 2020.

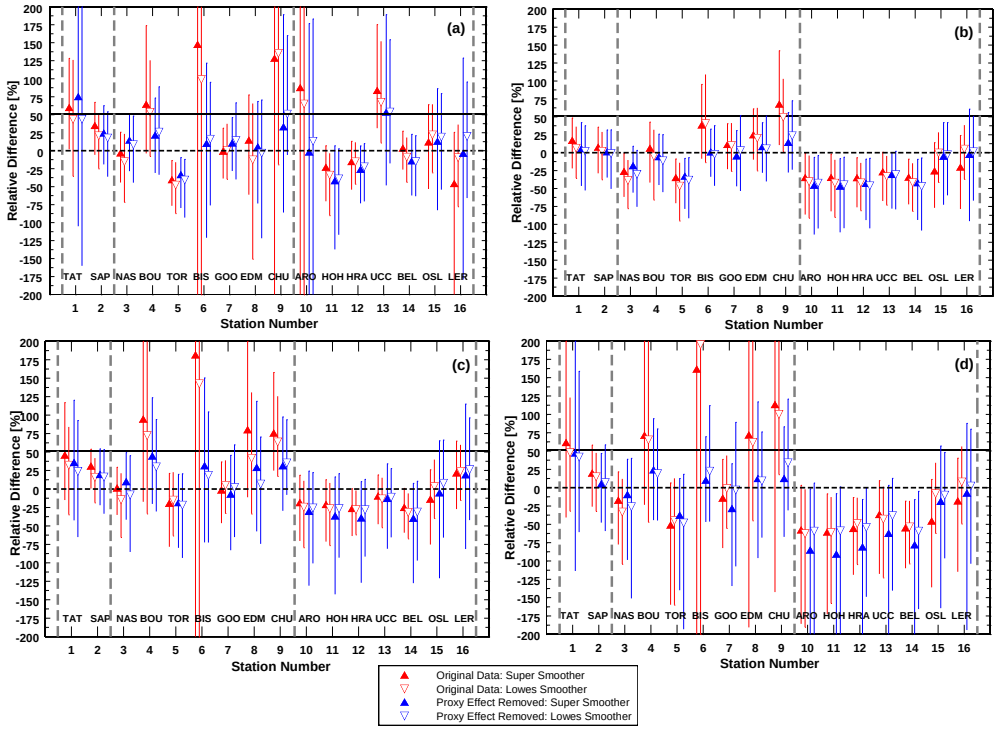

Figure 4. **The same as Fig. 3 but for the ozone recovery index, ORI_2(2020), based on Eq. (2).**

The ozone recovery is discussed for the original data (results in red in Figs. 3–4) and for the data with removed combined proxy signal (results in blue). Further in the text, the later data type will be called as the non-proxy data. A strong signal that the TCO_3 recovery at a selected station is slower (faster) than that found in the EESC pattern if the uncertainty ranges of both ORIs are below (above) the reference lines (i.e., 0 % for Figs. 3 and 51.7 % for Figs. 4) for all data types (WOUDC, MOD, MSR2, and MERRA2), regardless of the smoother type used.

For the original times series, the strong signal of slower TCO_3 recovery can be found for five stations: Nashville, Toronto, Hohenpeissenberg, Hradec Kralove, and Belsk. This is also in the non-proxy series for those stations excluding Nashville as the $ORI_1(2020)$ uncertainty range crosses the zero line when SS is used to smooth WOUDC data (Fig. 3a). In Arosa and Uccle, the slower ozone recovery is found in all datasets except WOUDC. This may suggest a problem with the homogeneity of WOUDC data at least for Arosa, as the results are different than those obtained at the nearby Hohenpeissenberg station. The slower TCO_3 recovery from the original data is identified in Oslo using all datasets except WOUDC.

The TCO_3 recovery faster than in the ESSC pattern only occurs at one station (Bismark). It can be found using $ORI_1(2020)$ from all original datasets except MOD. In addition, there are many individual cases where the localization of the uncertainty range of ORI estimate suggests significant difference between the TCO_3 and EESC recovery rates in at least one or two datasets. For example, this is the case for Sapporo for both ORIs derived from MOD data (Fig. 3b and Fig. 4b). The differences between ORIs values derived from the original and non-proxy series sometimes appear, e.g., both ORIs for Goose based on the original data show the slower recovery but the non-proxy data supports this only if $ORI_2(2020)$ is obtained from MOD (Fig. 4b).

A continuation of ozone decline after the turnaround in ODS concentration, which appears when the uncertainty range of $ORI_2(2020)$ is entirely below 0 regardless of the smoother type applied, is found both in the original and non-proxy time

https://doi.org/10.5194/acp-2022-680
Preprint. Discussion started: 10 October 2022

Atmospheric Chemistry and Physics Discussions

series from WOUDC (Toronto, see corresponding time series in Fig. 2b), MOD (Toronto, Arosa, Hohenpeissenberg, Uccle, Hradec Kralove, and Belsk), and MERRA2 data (Hohenpeissenberg, Hradec Kralove, and Belsk).

5 Discussion and conclusions

We proposed a novel tool to examine the stage of ozone recovery attributed to EESC changes. We introduce two ORIs. The first ORI is a difference between the TCO_3 value in 2020 and that in the year before the EESC maximum with the same EESC value as that in 2020. The second ORI is the percentage of the recovered ozone since the EESC maximum. The following ozone recovery phases can be identified when compared with the EESC change, i.e., faster, slower, nonconclusive (the hypothesis of the TCO_3 recovery driven entirely by EESC change cannot be rejected), and a continuation of TCO_3 decline after the EESC peak. For NH mid-latitudes in 2020, first three categories are found from the location of the ORI uncertainty ranges relative to the reference lines, $ORI_1(2020)$=0 % or $ORI_2(2020)$=51.7 %, which were obtained from the 1980-2020 EESC time series. The last category appears when the uncertainty range of ORI_2 is completely below 0 % reference line.

The stage of ozone recovery level was usually discussed comparing linear trend values before and after the year of the EESC overturning in the mid-1990s for the NH midlatitudes. The trends were obtained using MLR applied to various TCO_3 datasets and the slopes of the trend lines, which can be joint (Reinsel et al., 2005) or disjoint (Weber et al., 2018) at the EESC turning year, were compared. Weber et al. (2022) found that for the increasing rate of near global ozone (60°S-60°N) after 1995 was roughly a third of the decreasing rate calculated in the period 1978-1995 that corresponds with the ratio of the EESC change after and before the EESC maximum. This supports the success of MP and its further amendments. For this case, corresponding $ORI_2(2020)$ of ~47 % will be roughly estimated from the ratio between the TCO_3 trends (1/3) multiplied by the ratio between duration of the period after (24 yr.) and before (17 yr.) the EESC maximum. This estimate is close to the ODGI value in 2020 of 51.7% calculated for the NH mid-latitudes by Montzka et al. (2022). Then, two approaches, which are based on the TCO_3 trends and $ORI_2(2020)$, are almost equivalent and provide the TCO_3 recovery following EESC changes.

In our approach, to disclose phase of the ozone recovery, we compare ORIs, which are derived from the smoothed pattern of the ozone time series, with corresponding indicators of the mid-latitude EESC recovery. ORIs are calculated for each selected mid-latitudinal WOUDC station with the long time TCO_3 series. 16 stations are selected and various datasets for these stations based on the ground-based measurements, satellite overpasses, and two reanalyzes, are examined. The firm sign of the slower ozone recovery is identified for a group of neighborhood central/western Europe sites (Hohenpeissenberg, Hradec Kralove, and Belsk) and for Toronto as all ORI uncertainty ranges, regardless of the smoother type, are below the reference values obtained from the EESC change. The smallest uncertainty ranges of ORIs estimates are for the MOD dataset that result in the largest number of sites with slower TCO_3 recovery comparing with the EESC change.

A negative $ORI_2(2020)$ value means that the TCO_3 level in 2020 is lower than that in 1997 as the denominator in Eq. (2) is positive because the TCO_3 usually declined in NH mid-latitudes in the period 1980–1997. When the uncertainty range of $ORI_2(2020)$ is completely below zero, this means that the decline in ozone continues even after the EESC peak. This case is found for the group of central/western Europe stations from MOD and MERRA2 data. The continuation of ozone depletion in this region was previously discussed by Coldewey-Egbers et al. (2022) using merged satellite data.

Recent studies have focused on anthropogenic trends extracted by MLR to assess changes in the ozone layer by halogens, which implies parameterization of both trend and the natural ozone variability. In this study, two data types, the original and with the combined proxy effects removed, are under interests. The former is used to quantify changes in the UV radiation reaching the Earth's surface caused by ozone and the latter one is to delineate anthropogenic changes (due to man-made halogens) in the ozone layer. We only examine the TCO_3 means for the warm period of the year, since UVR levels are naturally high during this period, and if excessive UV exposure occurs due to lower TCO_3 values, it will cause serious consequences for health and the environment (Barnes et al., 2019). ORIs from the original and non-proxy datasets can sometimes be different,

https://doi.org/10.5194/acp-2022-680
Preprint. Discussion started: 10 October 2022

Atmospheric Chemistry and Physics Discussions

e.g., $ORI_2(2020)$ based on the Belsk's original MSR2 data shows a continuation of ozone decline, but the slower recovery stage comes from the non-proxy data (Fig. 4c).

The declining TCO_3 tendency in the original data (MOD and MERRA2) is revealed for the group of the central/western European stations for the entire period 1980-2020 using the original MOD and MERRA 2 dataset. In addition, the lower TCO_3 recovery rate appears in all datasets for this region. The ozone issue, which was raised in the early 1980s due to the anticipated UVR increase due to man-made halogens impact on the ozone layer, is still worth considering.

The variability of the ozone layer caused by the gradual removal of long-lived halogens from the stratosphere and changes in dynamic processes in the atmosphere, which are to some extent related to climate change, continue to pose a threat to the environment and health. The ozone recovery could be delayed (if it ever happens) in some isolated areas. This study is a kind of an introduction to use ORIs, which are based on the smoothed TCO_3 values in key EESC years, to monitor the current state of the ozone layer and its relationship with changes in man-made halogen loading in the stratosphere. We plan to use the ORI concept to discuss the ozone recovery globally from various gridded datasets.

Data availability. The TCO_3 data used in this study are taken from the WEB sources, listed in Table 2, with non-limited access. "Full model" version of MLR by Weber at al. (2022) is applied to remove "natural" variability form the original TCO_3 data. The MLR proxy set is taken from the WEB sources listed in their Table 2.

Author contributions. JK contributed to all aspects of the data analysis, manuscript preparation, and interpretation of the results.

Competing interests. The author declares that he has no conflict of interest.

Acknowledgments. We thank the Chief Inspectorate of Environmental Protection, Poland, for funding the ozone measurements at Belsk.

Funding. This work was supported by the Ministry of Science and Higher Education of Poland under Grant number 3841/E-41/S/2022.

References:

Arosio, C., Rozanov, A., Malinina, E., Weber, M., and Burrows, J.P.: Merging of ozone profiles from SCIAMACHY, OMPS and SAGE II observations to study stratospheric ozone changes, Atmos. Meas. Tech., 12, 2423–2444, https://doi.org/10.5194/amt-12-2423-2019, 2019.

Ball, W. T., Alsing, J., Mortlock, D. J., Staehelin, J., Haigh, J. D., Peter, T., Tummon, F., Stübi, R., Stenke, A., Anderson, J., Bourassa, A., Davis, S. M., Degenstein, D., Frith, S., Froidevaux, L., Roth, C., Sofieva, V., Wang, R., Wild, J., Yu, P., Ziemke, J. R., and Rozanov, E. V.: Evidence for a continuous decline in lower stratospheric ozone offsetting ozone layer recovery, Atmos. Chem. Phys., 18, 1379–1394, https://doi.org/10.5194/acp18-1379-2018, 2018.

Barnes, P.W., Williamson, C.E., Lucas, R.M, Robinson, S.A., Madronich, S., Paul, N.D., Janet F. Bornman, J.F., Bais, A.F., Sulzberger, B., Wilson, S.R., Andrady, A.L., McKenzie, R.L., Neale, P.J., Austin, A.T., Bernhard, G.H., Solomon, K.R., Neale, R.E., Young, P.J., Norval, M., Rhodes, L.E., Hylander, S., Rose, K.C., Longstreth, J., Aucamp, P.J., Ballaré, C.L., Cory, R.M., Flint, S.D., de Gruijl, Häder, D.P., Heikkilä, A.M., Jansen, M.A., Pandey, K.K., Robson, T.M., Sinclair, C.A., Wängberg, S., Worrest, R.C., Seyhan Yazar, S., Antony R. Young, A.R., and Richard G. Zepp, R.G.: Ozone depletion,

https://doi.org/10.5194/acp-2022-680
Preprint. Discussion started: 10 October 2022

Atmospheric Chemistry and Physics Discussions

ultraviolet radiation, climate change and prospects for a sustainable future, Nat Sustain., 2, 569–579, https://doi.org/10.1038/s41893-019-0314-2, 2019.

Bozhkova, V., Liudchik, A., and Umreiko, S.: Long-term trends of total ozone content over mid-latitudes of the Northern Hemisphere, Int. J. Remote Sens., 40, 5216–5229, https://doi.org/10.1080/01431161.2019.1579384, 2019.

Chehade, W., Weber, M., and Burrows, J. P.: Total ozone trends and variability during 1979–2012 from merged data sets of various satellites, Atmos. Chem. Phys., 14, 7059–7074, https://doi.org/10.5194/acp-14-7059-2014, 2014.

Chubachi, S.: Preliminary results of ozone observations at Syowa Station from February 1982 to January 1983, in: Proc. Sixth Symposium on Polar Meteorology and Glaciology, edited by: Kusunoki, K., vol. 34 of Mem. National Institute of Polar Research Special Issue, 13–19, 1984.

Cleveland, W. S.: Robust locally weighted regression and smoothing scatterplots. J. Am. Stat. Assoc., **74**, 829–836, https://doi.org/10.2307/2286407, 1979.

Coldewey-Egbers, M., Loyola, D. G., Lerot, C., and Van Roozendael, M.: Global, regional and seasonal analysis of total ozone trends derived from the 1995–2020 GTO-ECV climate data record, Atmos. Chem. Phys., 22, 6861–6878, https://doi.org/10.5194/acp-22-6861-2022, 2022.

Delage, O., Portafaix, T., Bencherif, H., Bourdier, A., and Lagracie, E.: The Empirical Adaptive Wavelet Decomposition (EAWD): An adaptive decomposition for the variability analysis of observation time series in atmospheric science, Nonlin. Processes Geophys., 29, 265–277, https://doi.org/10.5194/npg-29-265-2022, 2022.

Dietmüller, S., Garny, H., Eichinger, R., and Ball, W. T.: Analysis of recent lower-stratospheric ozone trends in chemistry climate models, Atmos. Chem. Phys., 21, 6811–6837, https://doi.org/10.5194/acp-21-6811-2021, 2021.

Farman, J. C., Gardiner, B. G., and Shanklin, J. D.: Large losses of total ozone in Antarctica reveal seasonal ClOx / NOx interaction, Nature, 315, 207–210, https://doi.org/10.1038/315207a0, 1985.

Friedman, J. H. 1984. A variable span smoother. Laboratory for Computational Statistics, Department of Statistics, Stanford University: Technical Report, SLAC-PUB-3477, https://doi.org/10.2172/1447470, 1984.

Harris, N. R. P., Kyrö, E., Staehelin, J., Brunner, D., Andersen, S.- B., Godin-Beekmann, S., Dhomse, S., Hadjinicolaou, P., Hansen, G., Isaksen, I., Jrrar, A., Karpetchko, A., Kivi, R., Knudsen, B., Krizan, P., Lastovicka, J., Maeder, J., Orsolini, Y., Pyle, J. A., Rex, M., Vanicek, K., Weber, M., Wohltmann, I., Zanis, P., and Zerefos, C.: Ozone trends at northern mid- and high latitudes – a European perspective, Ann. Geophys., 26, 1207–1220, https://doi.org/10.5194/angeo-26-1207-2008, 2008.

Komhyr, W.: Dobson spectrophotometer systematic total ozone measurement error, Geophys. Res. Lett., 7(2), 161–163, 1980.

Krzyścin, J.W., Rajewska-Więch, B. and Pawlak, J.: Long-Term Ozone Changes Over the Northern Hemisphere Mid-Latitudes for the 1979–2012 Period, Atmosphere-Ocean, 53:1, 153–160, https://doi.org/10.1080/07055900.2014.990869, 2015.

Krzyścin, J., Rajewska-Więch, B.: Specific variability of total ozone over Central Europe during spring and summer in the period 1979-2014. International Journal of Climatology, 36. 3539–3549, https://doi.org/10.1002/joc.4574, 2016.

Laine, M., Latva-Pukkila, N., and Kyrölä, E.: Analysing time-varying trends in stratospheric ozone time series using the state space approach, Atmos. Chem. Phys, 14, 9707–9725, https://doi.org/10.5194/acp-14-9707-2014, 2014

Mäder, J. A., Staehelin, J., Brunner, D., Stahel, W. A., Wohltmann, I., and Peter, T.: Statistical modeling of total ozone: Selection of appropriate explanatory variables, J. Geophys. Res., 112, D11108, https://doi.org/10.1029/2006JD007694, 2007.

Maillard Barras, E., Haefele, A., Stübi, R., Jouberton, A., Schill, H., Petropavlovskikh, I., Miyagawa, K., Stanek, M., and Froidevaux, L.: DLM estimates of long-term Ozone trends from Dobson and Brewer Umkehr profiles, Atmos. Chem. Phys. Discuss., https://doi.org/10.5194/acp-2022-344, in review, 2022.

Montzka, S.A., Dutton, G., and Vimont, I.: The NOAA Ozone Depleting Gas Index: Guiding Recovery of the Ozone Layer, https://gml.noaa.gov/odgi/, 2022. (last accessed 15 September 2022)

https://doi.org/10.5194/acp-2022-680
Preprint. Discussion started: 10 October 2022

Reinsel, G. C., Miller, A. J., Weatherhead, E. C., Flynn, L. E., Nagatani, R. M., Tiao, G. C., and Wuebbles, D. J.: Trend analysis of total ozone data for turnaround and dynamical contributions, J. Geophys. Res., 110, D16306, https://doi.org/10.1029/2004JD004662, 2005.

Sato, M., Hansen, J.E., McCormick, M.P. and Pollack, J.B.: Stratospheric aerosol optical depths, 1850-1990. J. Geophys. Res., 98, 22987–22994, https://doi.org/10.1029/93JD02553, 1993.

Solomon, S., Garcia, R. R., Rowland, F. S., and Wuebbles, D. J.: On the depletion of Antarctic ozone, Nature, 321, 755–758, https://doi.org/10.1038/321755a0, 1986.

Thompson, A. M., Stauffer, R. M., Wargan, K., Witte, J. C., Kollonige, D. E., and Ziemke, J. R.: Regional and seasonal trends in tropical ozone from SHADOZ profiles: Reference for models and satellite products, J. Geophys. Res.-Atmos., 126, e2021JD034691, https://doi.org/10.1029/2021JD034691, 2021.

van der A, R. J., Allaart, M. A. F., and Eskes, H. J.: Extended and refined multi sensor reanalysis of total ozone for the period 1970–2012, Atmos. Meas. Tech., 8, 3021–3035, https://doi.org/10.5194/amt-8-3021-2015, 2015.

Wald, A., and Wolfowitz, J.: On a test whether two samples are from the same population, Ann. Math. Stat., 11, 147–162, 1940.

Wargan, K., Labow, G.J., Frith, S.M., Pawson, S., Livesey, N.J., and Partyka, G.S.: Evaluation of the Ozone Fields in NASA's MERRA-2 Reanalysis. J. Clim, 30, 2961–2988. https://doi.org/10.1175/JCLI-D-16-0699.1, 2017.

Weber, M., Coldewey-Egbers, M., Fioletov, V. E., Frith, S. M., Wild, J. D., Burrows, J. P., Long, C. S., and Loyola, D.: Total ozone trends from 1979 to 2016 derived from five merged observational datasets – the emergence into ozone recovery, Atmos. Chem. Phys., 18, 2097–2117, https://doi.org/10.5194/acp-18-2097-2018, 2018.

Weber, M., Arosio, C., Coldewey-Egbers, M., Fioletov, V. E., Frith, S. M., Wild, J. D., Tourpali, K., Burrows, J. P., and Loyola, D.: Global total ozone recovery trends attributed to ozone-depleting substance (ODS) changes derived from five merged ozone datasets, Atmos. Chem. Phys., 22, 6843–6859, https://doi.org/10.5194/acp-22-6843-2022, 2022.